Computer Fraud and Security
ISSN (online): 1873-7056

The Equivalence Analysis of Image Matching Measure Functions in Digital Speckle Correlation Method

Liang Hong*
School of Media Engineering, Communication University of Zhejiang, Hangzhou 310018, China
**Corresponding Author*

Abstract:
Digital speckle correlation method (DSCM) is an import method of non- object image matching, has a lot of measure functions. The formulas have different physical meanings and application areas, each of which has good application examples. The author found, under certain conditions, some of the functions has obvious equivalence representation. In order to verify the above reasoning, the author makes a theoretical deduction from mathematics and establishes three equivalence classes of correlation coefficient formulas.. To validate the equivalence classes, a validation experiment was devised. Two parameters, namely the simple signal to noise ratio (*SSNR*) and the cross-sectional area at the bottom of the main peak (S_L), which most effectively reflect the shape of the measure function surface, were selected for the comparative analysis of the measure functions. The experimental results indicate that the two parameters, *SSNR* and S_L, of the measure functions within the same equivalence class are essentially equal and can be regarded as equivalent. The calculation times of each measure function within the same equivalence class were measured, and the optimal formula recommended for selection within the same equivalence class was presented. Based on the above conclusions, in the practices of image registration and image recognition, adopting the best function formula of the same type as the commonly used measure functions may potentially achieve the effect of a significant reduction in computational load while ensuring accuracy.

Keywords: digital speckle correlation method, measure function, equivalence class, non-object matching , simple signal to noise ratio

INTRODUCTION

Principle overview of the digital speckle correlation method:

Image matching (image recognition) can be generally divided into two situations: object-based recognition and non-object recognition. The so-called object is a collection of pixels that has specific image features (gray-level variation, contour, texture, etc.). Object-based recognition is relatively easy, and its matching measure function generally has a steep single peak. However, sometimes there are no obvious objects in the images that need to be compared, or due to the image being too blurry (or the template being too small), it is impossible to define recognizable objects in the template. For example, as shown in Figure 1, after uniformly spraying paint on the glass surface, its image consists of some random gray-level spots (generally called speckle patterns). When matching two speckle patterns containing the same content, since a single speckle does not contain sufficient distinguishable information and cannot be regarded as an object for search, only by increasing the comparison window and increasing the number of speckles within the window until it has sufficient distinguishable information can the matching be achieved. This kind of matching is a non-object recognition. In the field of optical measurement, the image matching function is generally calculated using a certain correlation measure, so this image matching method is called the Digital Speckle Correlation Method - DSCM (Digital Speckle Correlation Method) [1].

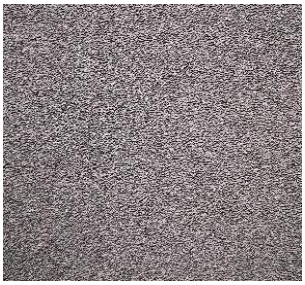

Figure 1. Artificial speckle image

Image matching based on regional gray levels can be mathematically described as follows:

As depicted in Figure 2, assume that I is the source image and f is the extracted image template from it. T represents the target image and g is its subdomain. When comparing the template and the target subdomain, the gray values at the corresponding points are respectively denoted as $f(i, j)$ and $g(i+u, j+v)$, where $u = k_1 - m_1$, $v = l_1 - n_1$, (u, v) are the relative displacement vectors between the images of g and f. Correspondingly, g can be expressed as $g_{(u,v)}$. According to a certain correlation algorithm, a correlation measure between the images can be established as ρ. The correlation measure value between g and f is calculated and denoted as $\rho(u, v)$. There are various algorithms for the measure based on image gray-level correlation [1]–[4]. For specific circumstances, by adopting an appropriate algorithm, the correlation measure function $\rho(u, v)$ can achieve superior graphical representation. Figure 3 shows the surface of a certain correlation measure function (C_{10}), which has a distinct single peak. The subdomain $g_{(u^*, v^*)}$ corresponding to the peak value precisely contains the same content as the template f.

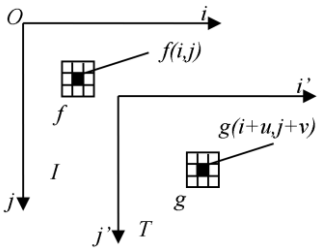

Figure 2. Source image and target image

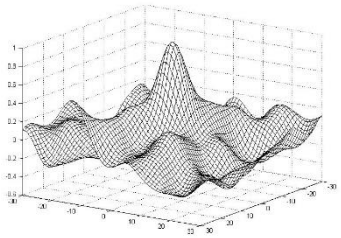

Figure 3. Surfaces of C_{10}

The disparities among various registration methods based on grayscale speckle images are primarily manifested in the differences of similarity measurement criteria. Based on distinct measurement criteria, numerous formulas to measure the correlation have been developed, as presented in Formulas (1) to (13) [2-6].

$$C_1 = -\sum\sum|f - g| \tag{1}$$

$$C_2 = -\sum\sum|f - \langle f\rangle - g + \langle g\rangle| \tag{2}$$

$$C_3 = -\langle|f - g|\rangle \tag{3}$$

$$C_4 = -\langle(f - g)^2\rangle \tag{4}$$

$$C_5 = \langle(f \cdot g)\rangle \tag{5}$$

$$C_6 = 1 - \frac{\sum\sum|f - g|}{\sum\sum f} \tag{6}$$

$$C_7 = 1 - \frac{\sum\sum (f-g)^2}{\sum\sum f^2} \tag{7}$$

$$C_8 = \frac{\sum\sum (f \cdot g)}{\sum\sum g^2} \tag{8}$$

$$C_9 = \frac{\sum\sum (f \cdot g)}{\sqrt{\sum\sum f^2} \cdot \sqrt{\sum\sum g^2}} \tag{9}$$

$$C_{10} = \frac{\sum\sum [(f-\langle f \rangle)\cdot(g-\langle g \rangle)]}{\sqrt{\sum\sum (f-\langle f \rangle)^2} \cdot \sqrt{\sum\sum (g-\langle g \rangle)^2}} \tag{10}$$

$$C_{11} = \frac{\langle f \cdot g \rangle - \langle f \rangle \cdot \langle g \rangle}{\sqrt{(\langle f^2 \rangle - \langle f \rangle^2) \cdot (\langle g^2 \rangle - \langle g \rangle^2)}} \tag{11}$$

$$C_{12} = \frac{N^2 \sum\sum (f \cdot g) - (\sum\sum f) \cdot (\sum\sum g)}{\sqrt{N^2 \sum\sum f^2 - (\sum\sum f)^2} \cdot \sqrt{N^2 \sum\sum g^2 - (\sum\sum g)^2}} \tag{12}$$

$$C_{13} = \frac{\left\{\sum\sum \left[(f - \langle f \rangle) \cdot (g - \langle g \rangle)\right]\right\}^2}{\sum\sum (f - \langle f \rangle)^2 \cdot \sum\sum (g - \langle g \rangle)^2} \tag{13}$$

Based on multiple considerations, researchers have put forward over ten measurement formulas for computing the similarity between the target sub-image and the template image. In specific DSCM engineering practices, one of them is typically selected empirically. Some of the abovementioned formulas may be equivalent. Jin Guanchang [3] demonstrated that $C_{10} = C_{11} = C_{12}$. Further discussions on the equivalence of these formulas are significant. It is also highly necessary to assess the reliability, validity, and efficiency of non-equivalent formulas in specific engineering applications of similarity measurement[7-11].

To assess the image registration measure function in DSCM, Liang HONG put forward an evaluation system [12]. The evaluation parameters within this system were mainly measured experimentally and did not involve excessive theoretical analysis.

MATERIALS AND METHODS

This paper will primarily analyze the above-mentioned 13 similarity measurement formulas from a mathematical viewpoint, dissecting the core mathematical contents of each formula. Based on the consistency of the core contents of each formula, corresponding equivalence classes will be established.

Under ordinary circumstances, the natural speckle field on the surface of rock specimens manifests the property of macroscopic uniformity and microscopic non-uniformity, whereas the artificial planar speckle field exhibits the characteristic of uniformity both macroscopically and microscopically [13 - 21]. For the sake of simplicity in the research, it is feasible to assume that the speckle field is uniform, that is, for different subdomains with sufficiently large areas, the following expressions that do not involve interaction operations between different images can be approximately regarded as constant values. Suppose

$$\sum\sum f \cong A_1 \ , \sum\sum f^2 \cong A_2 \ , \sum\sum g \cong B_1 \ , \sum\sum g^2 \cong B_2 \ , \langle f \rangle \cong \frac{A_1}{N} = A_3 , \langle g \rangle \cong \frac{B_1}{N} = B_3 ,$$
$$\sqrt{\frac{1}{N}\sum\sum (f - \langle f \rangle)^2} \cong \sigma_f \ , \sqrt{\frac{1}{N}\sum\sum (g - \langle g \rangle)^2} \cong \sigma_g \tag{14}$$

Then it follows that:

$$\begin{cases} C_1 = -\sum\sum |f - g| \\ C_3 = \frac{-1}{N}\sum\sum |f - g| = D_3 \sum\sum |f - g| \\ C_6 \cong C_6' = \frac{-1}{A_1}\sum\sum |f - g| + 1 = D_4 \sum\sum |f - g| + 1 \end{cases} \tag{15}$$

$$\begin{cases} C_4 = (\frac{-1}{N})\sum\sum (f - g)^2 = D_4 \sum\sum (f - g)^2 \\ C_7 \cong C_7' = \frac{-1}{A_2}\sum\sum (f - g)^2 + 1 = D_7 \sum\sum (f - g)^2 + 1 \end{cases} \tag{16}$$

$$\begin{cases} C_5 = \frac{1}{N}\sum\sum (f \cdot g) = D_5 \sum\sum (f \cdot g) \\ C_8 \cong C_8' = \frac{1}{B_2}\sum\sum (f \cdot g) = D_8 \sum\sum (f \cdot g) \\ C_9 \cong C_9' = \frac{1}{\sqrt{A_2 B_2}}\sum\sum (f \cdot g) = D_9 \sum\sum (f \cdot g) \\ C_{10} \cong C_{10}' = \frac{1}{N\sigma_f \sigma_g}\sum\sum (f \cdot g) - \frac{A_3 B_3}{\sigma_f \sigma_g} = D_{10} \sum\sum (f \cdot g) + E_{10} \\ C_{11} = C_{12} = C_{10} \end{cases} \tag{17}$$

In the aforementioned formulas, the parameters D_i and E_j are all constants.

Define σ_f and σ_g to respectively denote the gray standard deviations of the images $f = \{f(i, j)\}$ and $g = \{g(i', j')\}$, and let $\mathrm{Cov}(f, g)$ be the covariance of f and g. Through derivation, it can be obtained that:

$$C_{10} = C_{11} = C_{12} = \frac{\mathrm{Cov}(f, g)}{\sigma_f \sigma_g} = \mathrm{Corr}(f, g) = \mathrm{Corr}(u, v) \tag{18}$$

Wherein $\mathrm{Corr}(f, g)$ is the correlation coefficient of f and g.

Furthermore, evidently,

$$C_{13} = (C_{10})^2 \tag{19}$$

From the theory of signal processing, it is known that the information content of a signal remains invariant after simple translation and compression (or stretching). Thus, under the ideal assumption conditions for the aforementioned formulas, the following conclusions are presented:

① C_1, C_3, and C_6 are equivalent, with the core calculation being $\sum\sum|f-g|$. The set consisting of these three measure functions is termed *equivalence class I*, As shown in Formula (14).

② C_4 and C_7 are equivalent, with the core calculation being $\sum\sum(f-g)^2$. The set composed of these three measure functions is designated as *equivalence class II*, As shown in Formula (15).

③ C_5, C_8, C_9, C_{10}, C_{11},and C_{12} are equivalent, with the core calculation being $\sum\sum(f\cdot g)$. The set constituted by these three measure functions is named *equivalence class III*, As shown in Formula (16).

④ When the light intensity of the template and the target sub-domain does not vary significantly, C_2 is approximately equivalent to C_1.

The formulas within the same equivalence class are theoretically equivalent. It is only necessary to retain one or several with the least computational load, and the rest can be discarded. To verify the above conclusions, the following experiments were devised to conduct similarity evaluation and comparison of computational speed for the formulas within the same equivalence class.

Uniformly spray self-spraying paint on the glass surface to obtain a rough surface, as depicted in Figure 4. Images of the rough surface were captured to obtain speckle images as shown in Figure 1. For the convenience of theoretical analysis, considering the case without deformation and noise, both the source image *I* and the target image *T* adopt the image in Figure 1. A 40×40 pixel area is extracted from *T* as the template image *f*. Correlation measurements are performed on *f* and the sub-domain *g* of *I* using formulas (1)-(13) to obtain the corresponding graphs of each measure function. The shapes of the graphs corresponding to each measure function are similar to Figure 3, but there are distinctions in the height of the main peak, the width of the main peak, and the variance of the non-main peak region.

Figure 4. Glass plates with rough surfaces treated by spray painting

Based on the preceding analysis, the shapes of the measure function surfaces within the same equivalence class should exhibit high similarity after appropriate scaling operations (i.e., stretching or compression). To validate this hypothesis, we selected two parameters proposed by Liang HONG [12]: *SSNR* and C_L. The definitions of these parameters are as follows:

① $SSNR=\dfrac{C_m-\bar{C}}{\sigma_C}$ is the simple signal-to-noise ratio, where C_m is the maximum value of the correlation coefficient (theoretical or observed average value), $\bar{C}$ is the mean value of the correlation coefficient outside the main peak, and σ_C is the standard deviation of the correlation coefficient outside the main peak. The larger the *SSNR*, the more prominent the main peak, and the easier it is to detect the main peak.

$\bar{C}$ and σ_C are Corresponding to the system deviation and noise level during image matching. Therefore, they must be calculated after removing the main peak from the measurement function surface, as shown in Figure 5.

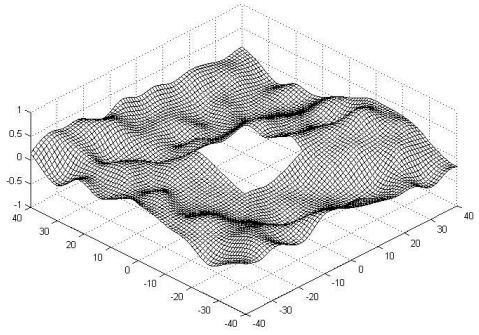

Figure 5. Surface with main peak removed

② S_L represents the cross-sectional area at the base of the main peak, as depicted in Figure 6. The curve constitutes a certain vertical section of the measurement function surface. By creating an iso-height section of the measurement function surface with a height of $C=C_L=\bar{C}+a_0\sigma_C$, the area of this section is S_L. The greater this index, the more effortless it becomes to search for the main peak. Based on the author's experience, $a_0 = 2.5$ can be adopted when the deformation of the specimen is minor; when the deformation of the specimen is significant or the image resolution is low, a_0=2.0 can achieve an excellent effect in screening the main peak. A larger S_L is beneficial for enhancing the speed of locating the main peak. In this experiment, $a_0 = 2.0$ was selected.

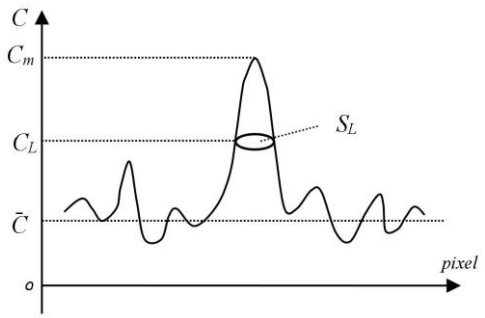

Figure 6. Correlation formular's performance parameters

If the *SSNR* and C_L parameters of two measure functions exhibit minimal differences, their shapes will also be highly similar. A 21×21-pixel region is randomly extracted from T to serve as the template image f. Based on this template, registration measures are calculated according to C_1 through C_{12}, resulting in the corresponding registration measure function surfaces. The *SSNR* and C_L parameters are then computed for each surface. This process is repeated 50 times, and the mean values $\overline{SSNR}$ and $\overline{C_L}$ are calculated. The results are summarized in Table 1.

Table 1. Evaluation Parameters of the Measure Functions

C_i	$\overline{SSNR}$	$\overline{C_L}(pixel)$	$\bar{t}(\mu s)$	C_i	$\overline{SSNR}$	$\overline{C_L}(pixel)$	$\bar{t}(\mu s)$
C_1	3.1810	11.93	29.3	C_5	3.325	40.06	50.8
C_3	3.0423	12.33	25.2	C_8	3.836	40.18	106.3
C_6	3.1918	12.07	33.8	C_9	3.764	40.37	152.1
C_2	2.8731	10.38	59.2	C_{10}	3.604	40.24	211.3
C_4	3.8271	15.36	32.4	C_{11}	3.692	40.10	177.5
C_7	3.6392	16.07	101.4	C_{12}	3.653	40.57	195.1

RESULTS

As shown in Table 1, the mean values of $SSNR$ and C_L , $\overline{SSNR}$ and $\overline{C_L}$ for the measurement functions C_5, C_8, C_9, C_{11}, and C_{12} exhibit minimal differences. This indicates that the surface shapes of these five measurement functions are highly similar, thereby validating our conclusion that they belong to the same equivalence class. Similarly, the results support the classification of C_1, C_3, and C_6 into one equivalence class, as well as C_4 and C_7 into another. Additionally, the values of $\overline{SSNR}$ and $\overline{C_L}$ for C_2 and C_1 show negligible differences. Under reasonable assumptions, C_2 can be considered approximately equivalent to C_1.

Furthermore, Formula C_{13} is derived by squaring Formula C_{10}. The author argues that C_{13} lacks practical value for the following reasons: C_{13} represents a nonlinear transformation of Formula C_{10}, which can be viewed as a nonlinear filtering of the associated measure function. This transformation sharpens the main peak and suppresses secondary peaks of the measure function surface to some extent, effectively acting as a peak selection mechanism. However, theoretically, C_{13} does not provide additional information beyond what is contained in C_{10}. Moreover, the shape of the main peak in surfaces fitted using C_{13} data exhibits directional distortion, leading to significant systematic errors in sub-pixel interpolation. Therefore, it is not advisable to adopt C_{13} for practical applications.

DISCUSSION

Theoretically, the measure functions within the same equivalence class are equivalent in terms of their mathematical properties but differ only in their representational forms. Selecting any one of them does not affect the outcome or precision of the registration process. In practical engineering applications, it is sufficient to choose a single measure function from each equivalence class for registration measurements. It is recommended to select the function with the highest computational efficiency to optimize processing time. As shown in Table 1, the calculation speeds of C_1, C_3, and C_6 in *equivalence class I* are comparable, and any of these can be chosen without impacting performance. In *equivalence class II*, C_4 exhibits significantly faster computation times compared to C_7, making C_4 the preferred choice. In *equivalence class III*, C_5 demonstrates superior computational speed relative to C_8, C_9, C_{10}, C_{11} and C_{12}, and thus C_5 should be selected for optimal performance.

ACKNOWLEDGMENTS

This work was supported by Natural Science Foundation of China No. 61671404.

REFRENCES

[1] Irani M, Anadan P. All about direct methods. Proceedings of International workshop Vision Algorithms, Corfu, Greece: IEEE Press, 1999: 267-277.

[2] Bamea D I, Silverman H F. A class of algorithms for fast digital image registration . IEEE Transactions on Computing, 1972, 21(2): 179-186.

[3] Jin G C.Computer-Aided Optical Metrology(2e). Beijing: Tsinghua University Press, 2007. 142, 146, 147. (in Chinese).

[4] Rosenfeld A, Kak A C. Digital picture processing . New York: Academic Press, 1982.

[5] Prat W K. Digital Image Processing. New York: Wiley Press, 1991.

[6] MA Shao-peng, JIN Guan-chang, PAN Yi-shan. Study on the White Light DSCM Method for Deformation Measurement of Rock Materials . JOURNAL OF EXPERIMENTAL M ECHANICS. 2002, 17(1): 10-16.

[7] Xinyu Wang, Liang Hong. The Research on Wildebeest Effect Based on MBTE Model. Frontiers in Humanities and Social Sciences. 2024, 4(7): 214-219.

[8] Yi Dong, Liang Hong, GuiRong Wang. Research and Analysis on Key Techniques of Digital Speckle Correlation Method. Journal of Physics: Conference Series (CISAT 2019). 1345 (2019) 022042.

[9] Qiang Chen, Zhixin Tie, Liang Hong, Youtian Qu, Dengwen Wang. Improved Search Algorithm of Digital Speckle Pattern Based on PSO and IC-GN. Photonics. 2022, 9, 167.

[10] DONG Yi, WANG Guirong, HONG Liang. Digital image correlation sub-pixel displacement solving algorithm based on improved gradient method. Modern Electronics Technique. 2022, 45(17): 29-34.

[11] Xuemei Wang, Guili Tao, Xuelan Zou, Liang Hong. Inverse Covariance Intersection Fusion Steady-state Kalman Filter for Uncertain Systems with Missing Measurements and Linearly Correlated White Noises. Proceedings of the 40th Chinese Control Conference. 2021, shanghai, China. 3209-3213.

[12] Liang HONG. Grayscale image DSCM matching algorithm evaluation system. Application Research of Computers, 2015, 32 (01): 262-264, 268.

[13] Siripon Kaoroptham, Rittipol Chantarat, & Prapot Kunthong. (2024). Using Digital Image Correlation (DIC) in MATLAB Monitoring Number and Size of Speckle Granules. Science & Technology Asia, 29(2), 63–73.

[14] Dale Zhang, Gang Huang, Ledi Li, Shengnan He, Yong Su, Shenghong Huang, Menglai Jiang, and Weihua Wang, "Preprocessing methods for reducing the impact of image decorrelation in laser speckle digital image correlation," Opt. Continuum 4, 476-487 (2025).

[15] Huang Gang, Zhang Wuji, He Shengnan, Su Yong, Pan Zhiwei, Huang Shenghong, Wang Weihua, Zhang Dale. Quality assessment of laser speckle image sequences for digital image correlation by Sequence-image Quality Evaluation Index. Measurement. Volume 229, 2024, 114486.

[16] Yahong Feng, Lianpo Wang. Stereo-DICNet: An efficient and unified speckle matching network for stereo digital image correlation measurement, Optics and Lasers in Engineering, Volume 179, 2024, 108267.

[17] Liu, L, Niu, B, Xu, Z. et al. A digital speckle stereo matching algorithm based on epipolar line correction. Signal, Image and Video Processing, 4579–4588 (2024).

[18] Yuzhe Tian, Cheng Zhao, Jinquan Xing, Jialun Niu, Yuan Qian. A new digital image correlation method for discontinuous measurement in fracture analysis. Theoretical and Applied Fracture Mechanics, Volume 130, 2024, 104299.

[19] Mikael Sjödahl and Pascal Picart, "Refocus criterion from image-plane speckle correlation in digital holographic interferometry," Appl. Opt. 63, B104-B113 (2024).

[20] Dan Wu, Lingxiao Yin, Yuan Gao, Zhifei Miao, Yifan Wang. Internal crack detection based on thermal excitation enabled digital image correlation method. Measurement, Volume 227, 2024, 114262.

[21] Woodland, S.K, Gagnon, É, Packulak, T.R.M. et al. Paint Speckle Application Recommendations for Digital Image Correlation Analysis of Brazilian Tensile Strength Tests on Low-Porosity Rocks. Rock Mech Rock Eng 57, 1495–1507 (2024).